Electronic Supplementary Material (ESI) for Materials Advances.
This journal is © The Royal Society of Chemistry 2020

Supporting Information for

Structure dependent photostability of ITIC and ITIC-4F

Laura Ciammaruchi,[*a] Osnat Zapata-Arteaga,[a] Edgar Guitierrez,[b] Jaime Martín[b,c] and Mariano Campoy-Quiles[*a]

[a] Institute of Materials Science of Barcelona (ICMAB-CSIC), Campus of the UAB, 08193, Bellaterra, Spain

[b] POLYMAT and Polymer Science and Technology Department, Faculty of Chemistry, University of the Basque Country UPV/EHU, Manuel de Lardizabal 3, 20018, Donostia-San Sebastián, Spain

[c] Ikerbasque, Basque Foundation for Science, E-48011, Bilbao, Spain

*Corresponding authors. E-mails: lciammaruchi@icmab.es; mcampoy@icmab.es

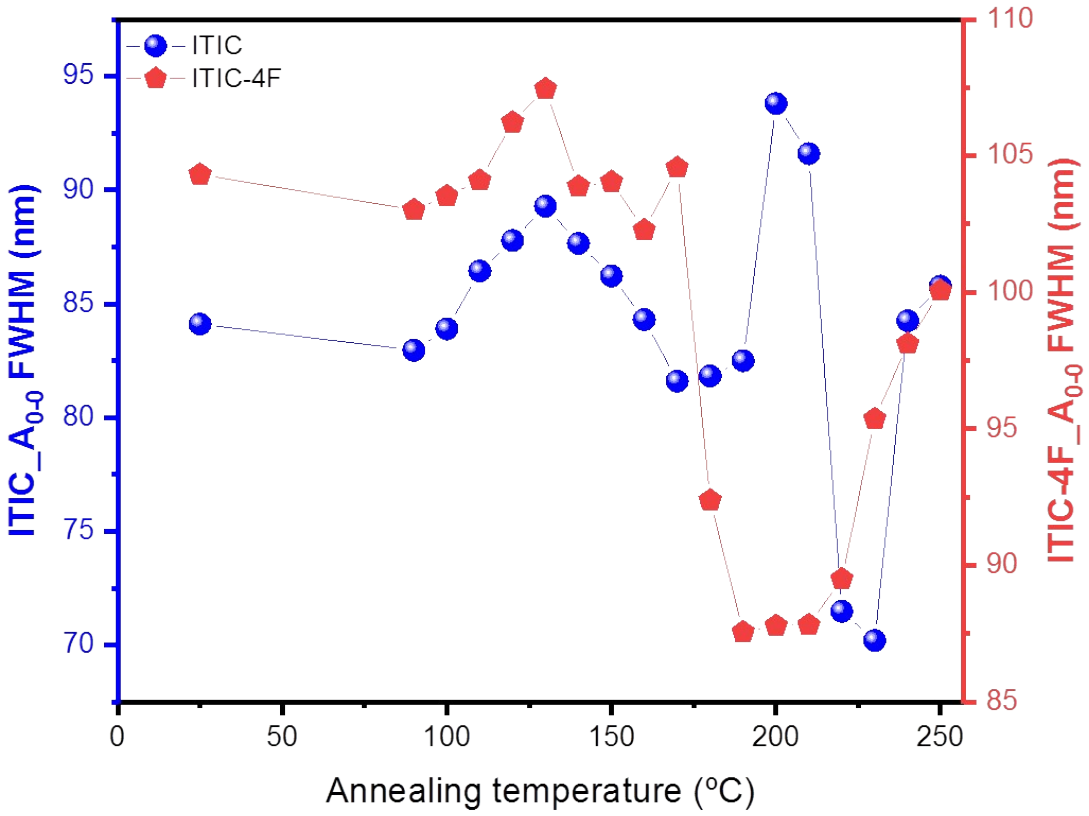

Figure S1. Full-Width-Half-Maximum (FWHM) values as function of the annealing temperatures. Values extrapolated from UV-vis absorption data for ITIC (balloon) and ITIC-4F (pentagon).

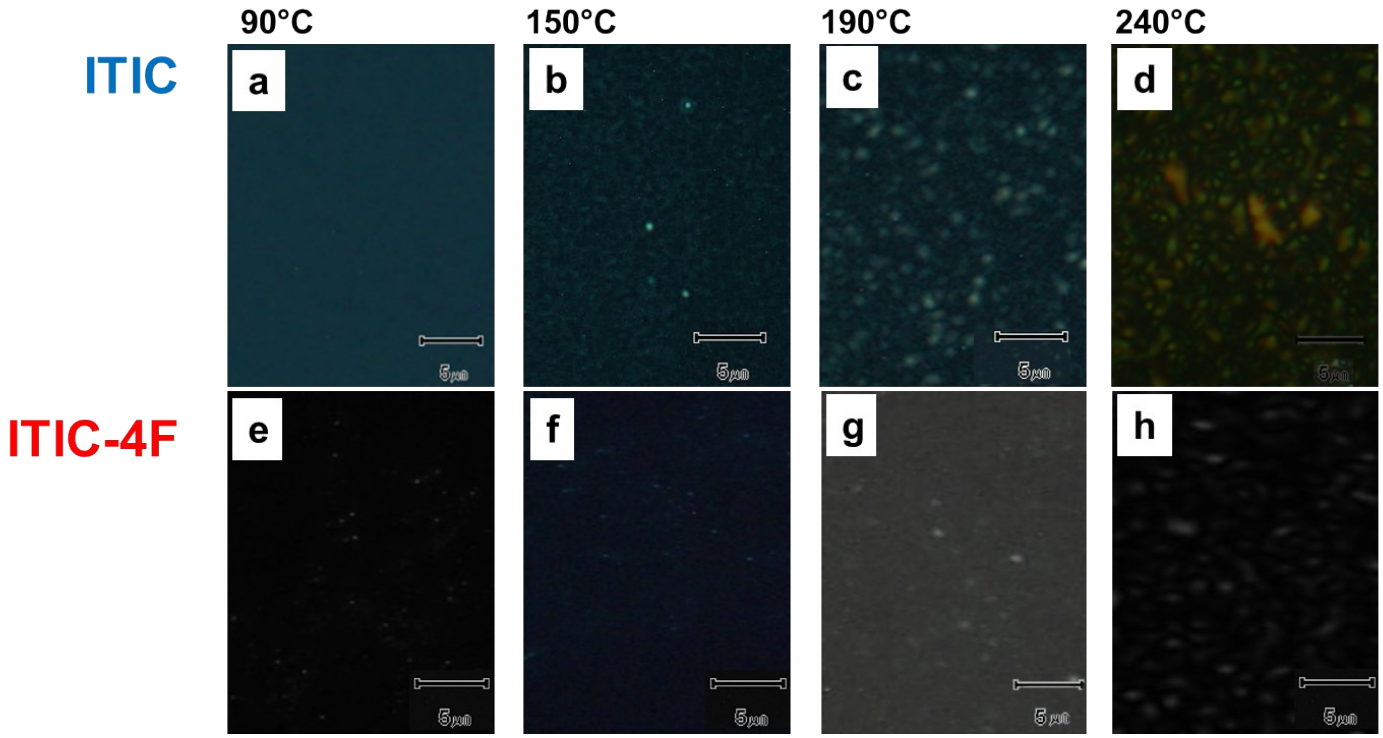

Figure S2. Polarized optical microscopy images of ITIC (upper row) and ITIC-4F (lower row) thin films deposited on ITO-covered glass and annealed at 90°C (a,e), 150°C (b,f), 190°C (c,g) and 240°C (d,h).

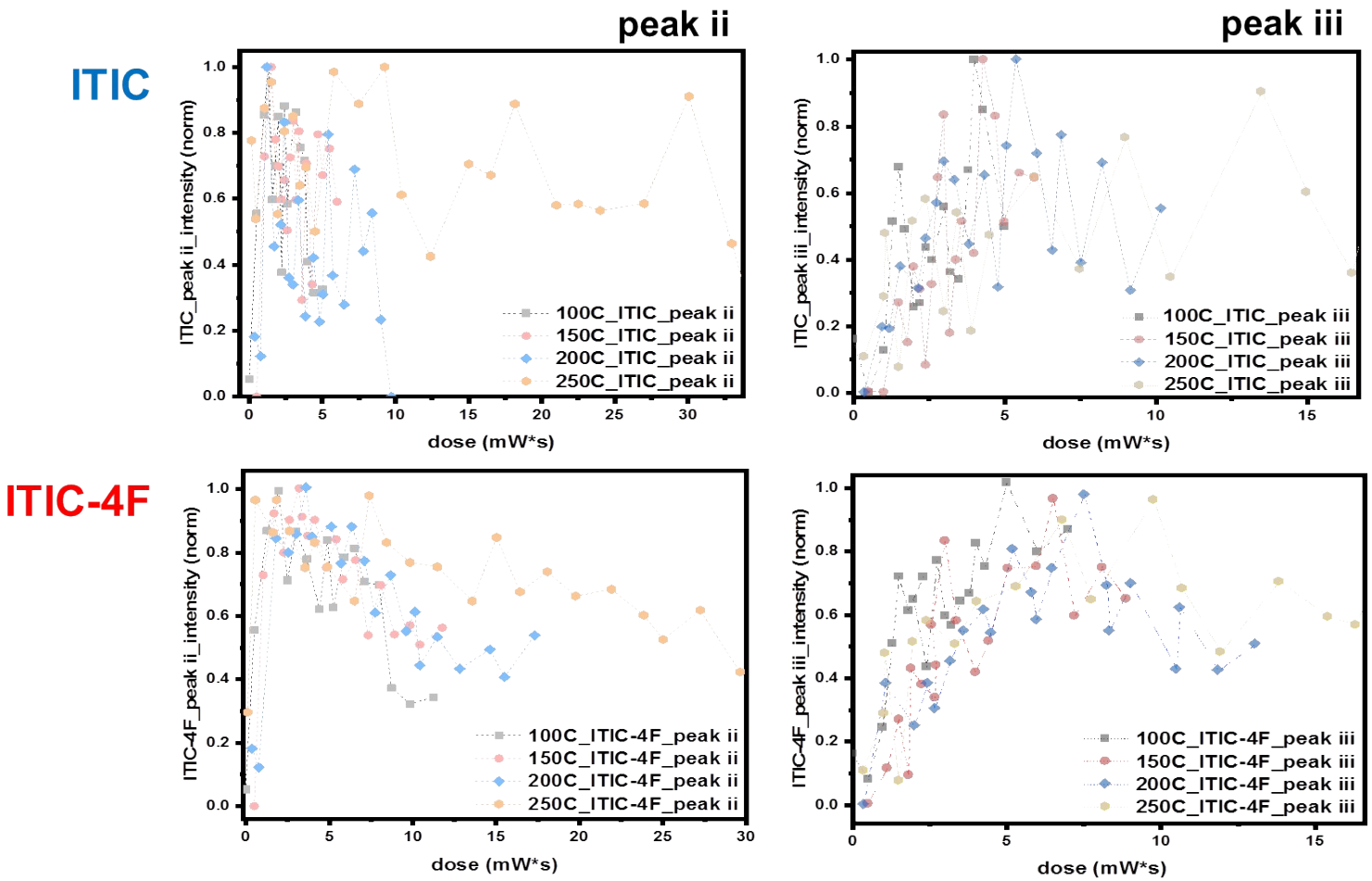

Figure S3. Dose-dependent Raman decay for peaks ii and iii, for ITIC (upper row) and ITIC-4F (lower row) annealed at different temperatures.

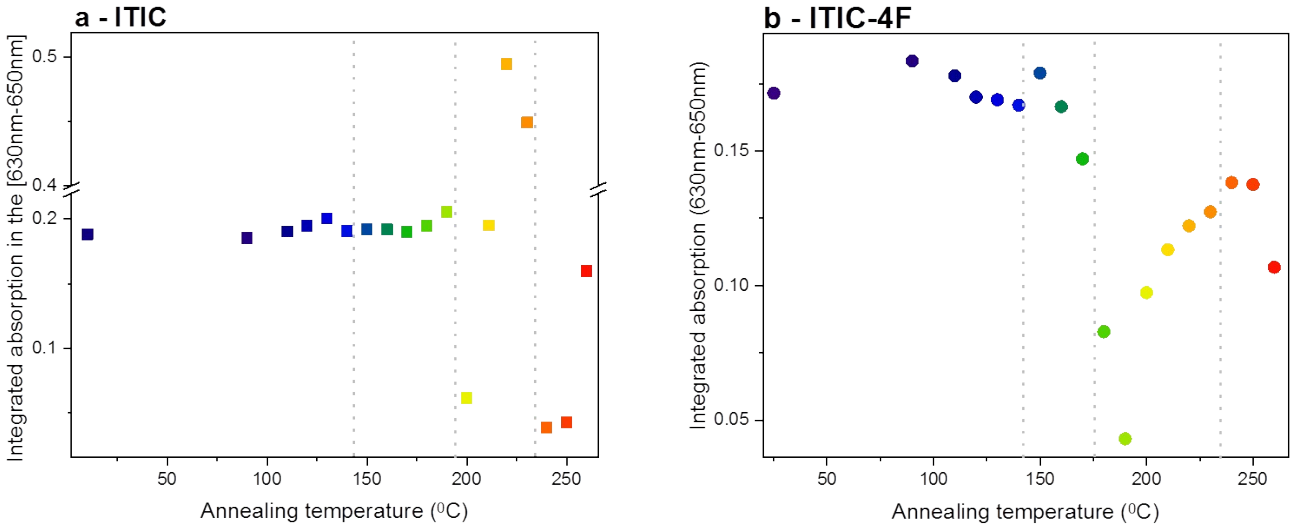

Figure S4. Integrated absorption values in the (630nm-650nm) range against the materials' annealing temperature, for ITIC (a) and ITIC-4F (b).

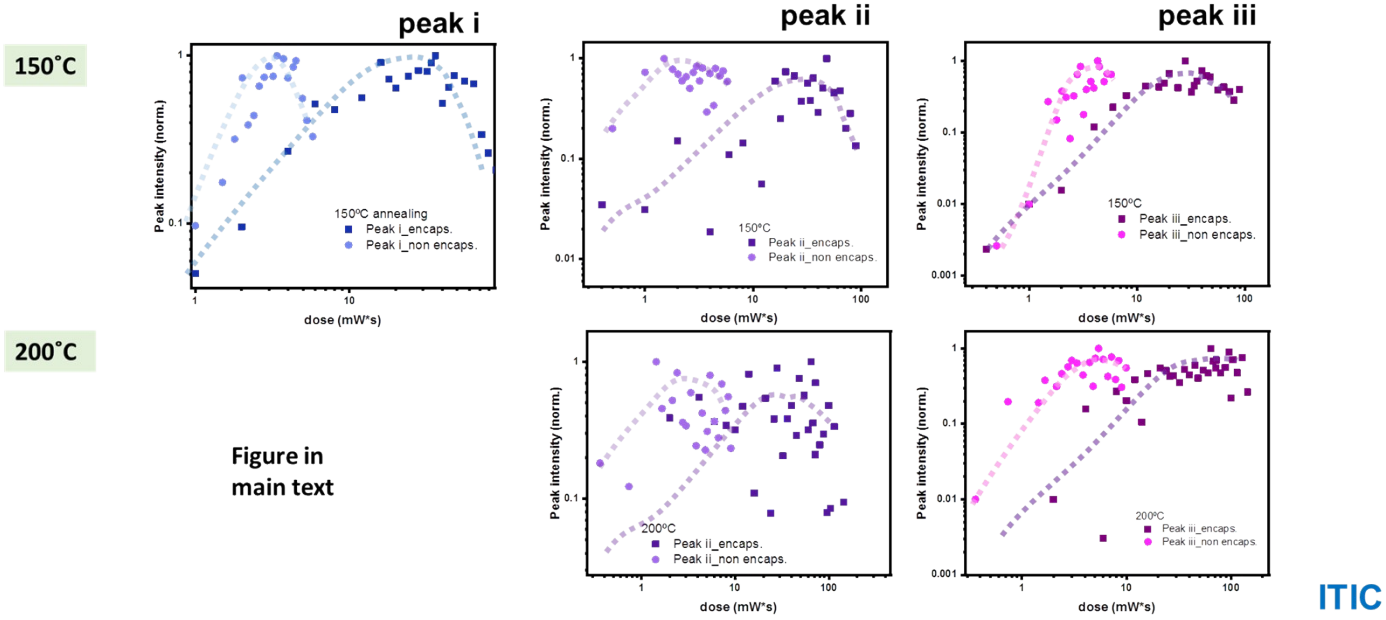

Figure S5. Dose-dependent Raman decay for peaks i, ii and iii, for encapsulated ITIC annealed at 150°C (upper row) and 200°C (lower row). Dashed lines are just a guide for the eye.

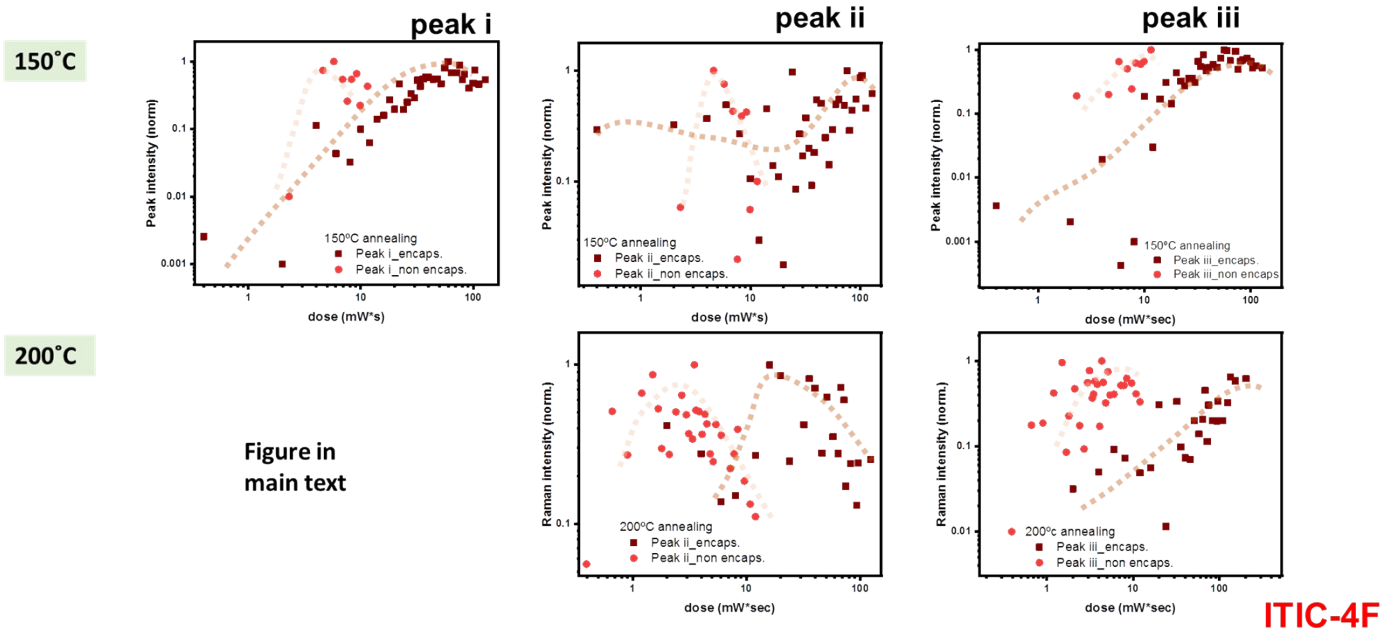

Figure S6. Dose-dependent Raman decay for peaks i, ii and iii, for encapsulated ITIC-4F annealed at 150°C (upper row) and 200°C (lower row). Dashed lines are just a guide for the eye.

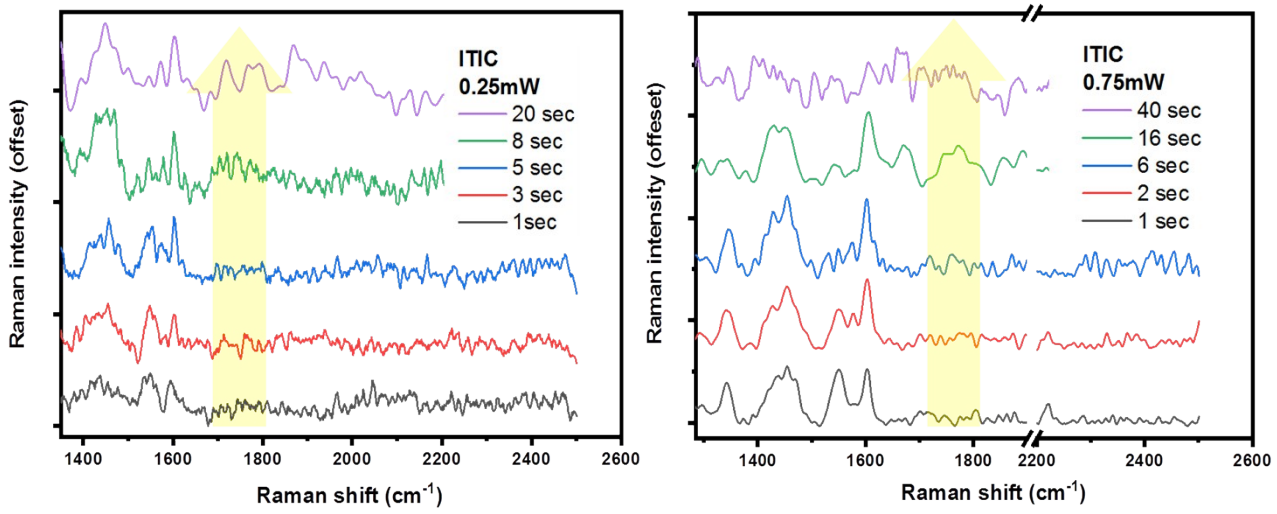

Figure S7. Raising vibrational mode in the (1700 cm^{-1} - 1850 cm^{-1}) range, for ITIC probed at two different powers.

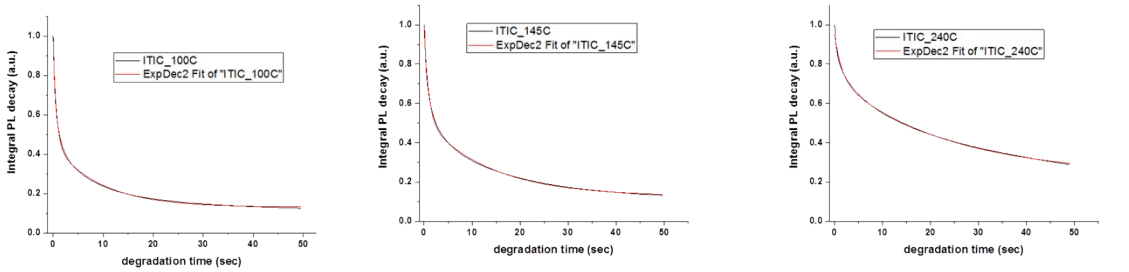

Model	ExpDec2	Model	ExpDec2
Equation	y = A1*exp(-x/t1) + A2*exp(-x/t2) + y0	Equation	y = A1*exp(-x/t1) + A2*exp(-x/t2) + y0
Plot	L26A_PL_0.25mW_sum centered at 760	Plot	ITIC_27A
y0	0.12991 ± 5.10095E-4	y0	0.12653 ± 7.79248E-4
A1	0.543 ± 0.00404	A1	0.47956 ± 0.00334
t1	0.43425 ± 0.00948	t1	0.53277 ± 0.01293
A2	0.32031 ± 0.00204	A2	0.39043 ± 0.00163
t2	2.74175 ± 0.09702	t2	2.61992 ± 0.12758
Reduced Chi-Sqr	3.13237E-5	Reduced Chi-Sqr	2.78028E-5
R-Square (COD)	0.99743	R-Square (COD)	0.99842
Adj. R-Square	0.99741	Adj. R-Square	0.99841

Model	ExpDec2		
Equation	y = A1*exp(-x/t1) + A2*exp(-x/t2) + y0		
Plot	ITIC_28B		
y0	0.23753 ± 0.00194		
A1	0.22117 ± 0.00265		
t1	0.44474 ± 0.03692		
A2	0.48914 ± 0.00128		
t2	4.45672 ± 0.26832		
Reduced Chi-Sqr	2.34368E-5		
R-Square (COD)	0.99877		
Adj. R-Square	0.99876		

ITIC

Figure S8. Fitting curves and parameters for ITIC integrated PL decay curve under *in-situ* 633nm laser degradation, for three sample annealing temperatures.

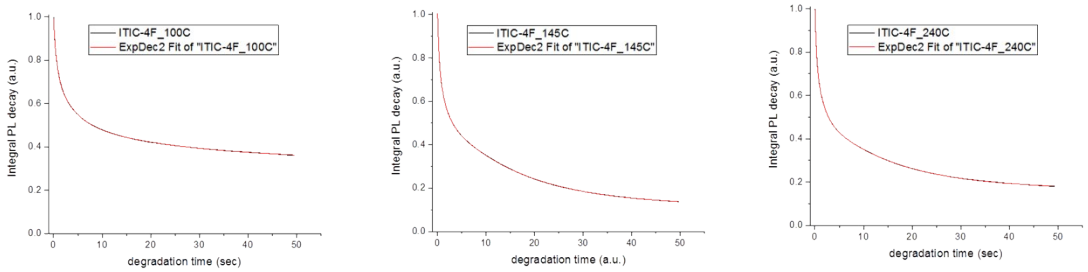

Model	ExpDec2	Model	ExpDec2
Equation	y = A1*exp(-x/t1) + A2*exp(-x/t2) + y0	Equation	y = A1*exp(-x/t1) + A2*exp(-x/t2) + y0
Plot	ITIC-4F_31A	Plot	ITIC-4F_32A_0.25mW_785 sum
y0	0.33684 ± 8.71231E-4	y0	0.11944 ± 1.78346E-4
A1	0.23921 ± 0.00178	A1	0.19257 ± 0.00294
t1	3.67161 ± 0.00666	t1	1.29745 ± 0.00524
A2	0.22879 ± 0.00135	A2	0.25895 ± 0.00282
t2	2.74175 ± 0.04881	t2	2.61992 ± 0.01302
Reduced Chi-Sqr	9.89952E-7	Reduced Chi-Sqr	7.30322E-7
R-Square (COD)	0.99989	R-Square (COD)	0.99996
Adj. R-Square	0.99989	Adj. R-Square	0.99996

Model	ExpDec2		
Equation	y = A1*exp(-x/t1) + A2*exp(-x/t2) + y0		
Plot	ITIC-4F_33B		
y0	0.1682 ± 1.4818E-4		
A1	0.2 ± 0.00195		
t1	1.41192 ± 0.00359		
A2	0.27846 ± 0.00179		
t2	4.45672 ± 0.00997		
Reduced Chi-Sqr	5.3057E-7		
R-Square (COD)	0.99996		
Adj. R-Square	0.99996		

ITIC-4F

Figure S9. Fitting curves and parameters for ITIC-4F integrated PL decay curve under *in-situ* 633nm laser degradation, for three sample annealing temperatures

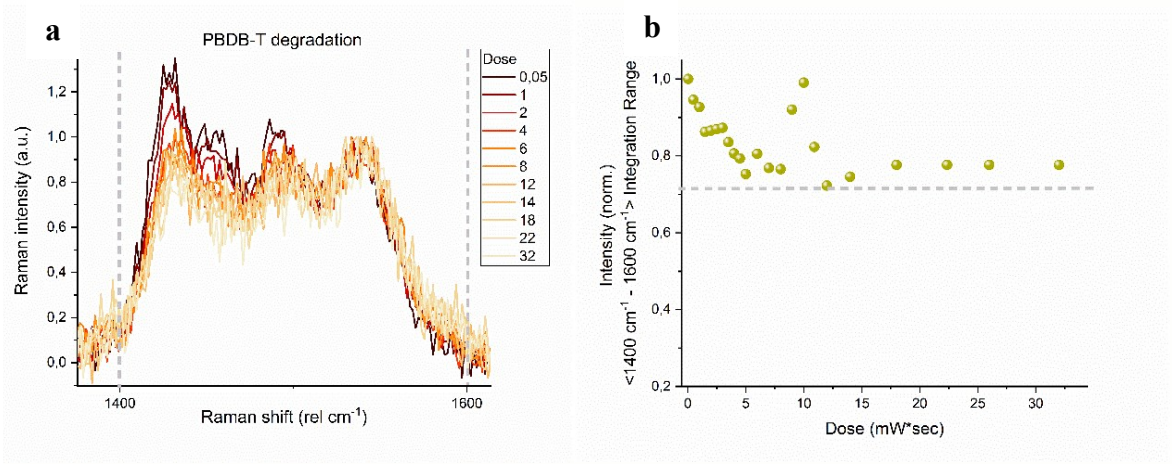

Figure S10. (a) Raman intensity signal acquired with a 488nm laser at different dose intakes, for a PBDB-T donor thin film deposited on top of ZnO. (b) Integrated PBDB-T Raman intensity in the (1400 cm^{-1}-1600 cm^{-1}) range as a function of the received dose.